Evolution Mechanism of Heterointerface Cross-section during Growth of GaAs Ridge Quantum Wires by Selective Molecular Beam Epitaxy

Taketomo Sato*, Isao Tamai, Souichi Yoshida and Hideki Hasegawa
Research Center for Integrated Quantum Electronics and Graduate School of Electronics and Information Engineering, Hokkaido University, North-13, West-8, Sapporo 060-8628, JAPAN

Abstract

The mechanism determining heterointerface cross-sections is studied for GaAs ridge quantum wires (QWRs) grown by selective molecular beam epitaxy (MBE). Arrays of $<\bar{1}10>$- and $<\bar{1}\,\bar{1}2>$-orientated QWRs were grown on (001) and (111)B GaAs patterned substrates, respectively. A detailed investigation of cross-sections of wires has shown that the boundary planes appear on both sides of QWRs, keeping a constant angle, θ with respect to the flat top of the substrate pattern, and they determine the lateral wire width. Their evolution mechanism has turned out to be a kinetic process, reflecting differences in migration and atom incorporation rates on different facets. Simple formulas for θ have been derived, and they have shown excellent agreements with experiment. This has led to precise kinetic control of the wire width by growth conditions.

PACS codes: 81.07.Vb, 81.16.Dn
Keywords: selective growth, molecular beam epitaxy (MBE), patterned substrate, growth mechanism, GaAs

*Corresponding author. Fax: +81-11-716-6004, e-mail: taketomo@rciqe.hokudai.ac.jp

1. Introduction

Selective molecular beam epitaxy (MBE) / metal organic vapour phase epitaxy (MOVPE) of III-V semiconductor heterointerfaces on pre-patterned substrates is one of the most promising techniques for the formation of position- and size-controlled arrays of quantum wires (QWRs) and quantum dots (QDs) [1-4]. Recently, we have reported that $<\bar{1}10>$-oriented QWRs can be successfully formed on (001) patterned substrates by a selective MBE growth for both InP- [5] and GaAs-based materials [6,7]. However, growth on non-planar substrates is complicated due to the simultaneous involvement of various high-index facets and related kinetic processes. Actually, the cross-sectional features of grown QWRs were quite different in various orientations of patterned substrates. For precise control of the feature size, proper understanding of the underlying growth mechanism for various crystal orientations is inevitable.

The purpose of this paper is to clarify the mechanism which determines heterointerface cross-sections of GaAs ridge QWRs grown by selective MBE process. From a new understanding of the growth mechanism, precise control of the wire width has been realized for both $<\bar{1}10>$- and $<\bar{1}\,\bar{1}2>$-oriented wires grown on (001) and (111)B patterned substrates, respectively.

2. Experimental

In this paper, two kinds of QWRs were grown by selective MBE on patterned substrates. Arrays of $<\bar{1}10>$- and $<\bar{1}\,\bar{1}2>$-oriented mesa stripes shown in **Fig. 1(a)** were formed on semi-insulating (001) GaAs substrates and on (111)B GaAs substrates, respectively, by a standard lithography and wet etching process. After surface treatment in the atmosphere, thermal cleaning under arsenic pressure was done in the MBE chamber just before the growth.

A typical material supply and the growth sequence are shown in **Fig. 1(b)** and **(c)**, respectively. First, GaAs ridge structures were grown on the patterned substrates. Then, $Al_{0.3}Ga_{0.7}As/GaAs/Al_{0.3}Ga_{0.7}As$ layers were supplied on the ridge structures, and this led to the formation of embedded GaAs wires. The growth rate of the AlGaAs layer kept to be 1000 nm/hour in terms of the value for growth on a planar substrate. The V/III flux ratio was set at 30 for the growth on the (001) substrate and 10 for the growth on the (111)B substrate, respectively. Substrate temperature was changed within the range from 600˚C to 680˚C.

3. Results and discussion

3.1 Growth of <$\bar{1}$10>- and <$\bar{1}\bar{1}$2>-oriented wires and boundary planes

Figures 2(a) and (b) show cross-sectional SEM images of <$\bar{1}$10>- and <$\bar{1}\bar{1}$2>- oriented QWRs formed on (001) and (111)B patterned substrates, respectively. After the stain etching by alkali solution, complex features due to the growth of heterointerfaces became visible.

In the case of the growth on the <$\bar{1}$10>-oriented mesa, the arrow-head shaped nano-wire was selectively formed on the top (113) facets of the GaAs ridge structure, as shown in **Fig. 2(a)**. Furthermore, two facet boundary planes separating (111)/(113) growth region became also visible within the AlGaAs layer after the stain etching.

On the other hand, growth of GaAs ridge on <$\bar{1}\bar{1}$2>-oriented mesa stripes led to formation of flat-top ridge structures defined by the top (111)B plane and side (5-12) facets. As shown in **Fig. 2(b)**, subsequent AlGaAs/GaAs/AlGaAs supply resulted in the self-organized formation of QWRs on the top plane with decreased sizes. In this case, boundary planes were not visible.

However, repeated growth experiments indicated the formation of facet boundary planes in the bottom AlGaAs layers in both cases, as shown in **Figs. 3(a) and (b)** respectively for the <$\bar{1}$10>- and <$\bar{1}\bar{1}$2>-oriented wires. The lateral wire width reduced by following the facet boundary planes for both orientations. Furthermore, it was found that the angle of the facet boundary planes, θ, kept a constant value with respect to a flat top of the mesa throughout the entire growth. The reason why the facet boundary planes became visible after the light etching for the <$\bar{1}$10>-wire, whereas they were not visible in the <$\bar{1}\bar{1}$2>-wire is related to the composition change of AlGaAs ridge. Namely, the composition of AlGaAs layer slightly changed between on (111) and (113) facets for growth on the (001) substrate, while it remained unchanged across the (111)B/(5-12) boundary for growth on the (111)B substrate.

3.2 Evolution mechanism of facet boundary planes

At first, one might think that the high-index boundary planes themselves correspond to particular crystalline facets activated during growth. However, detailed measurements has shown that it is not case. In fact, their directions were found to depend strongly on the growth temperature, T_{sub}, as shown in **Fig. 4** for <$\bar{1}$10>- and <$\bar{1}\bar{1}$2>-oriented wires.

Figure 5 shows our model for evolution of the facet boundary planes. Here, it is assumed that growth rates of AlGaAs are different between on the top and side facets of ridge structures. Then, from the simple geometrical consideration, the boundary angle, θ, should satisfy the following relation, as first derived for growth on (001) substrates [7].

$$\tan\theta = \frac{\alpha \cdot \tan\theta_{side} - \tan\theta_{top}}{\alpha - 1} \qquad (1)$$

Here, α is the growth rate ratio defined as $\alpha = t_{top} / t_{side}$, where t_{top} is the vertical growth rate on the top facet and t_{side} is that on the side facet. θ_{top} and θ_{side} are the angles of the top facet and the side facet with respect to a flat top of mesa, respectively. For example, the value of $\theta_{top} = 25.2^{\circ}$ and $\theta_{side} = 54.7^{\circ}$ should be used for <$\bar{1}$10>-oriented wires as the angle of top (113) facet and side (111) facets, respectively. In the case of <$\bar{1}\bar{1}$2>-oriented wire on (111)B

substrate, the value of $\theta_{top} = 0^{\circ}$ and $\theta_{side} = 50.8^{\circ}$ should be used as the angle of the top (111)B plane and the side (5-12) facets. Thus, this formulas should be applicable to various QWRs having different facet orientations.

3.3 Control of lateral wire size by facet boundary planes

In order to confirm our hypothesis, growth rates on the top and side facets of the GaAs ridge structure were investigated for various substrate temperatures. The measured values of the normalized vertical growth thicknesses, t_{top} and t_{side}, as defined in **Fig. 5** are plotted in **Fig. 6** as a function of the growth temperature, T_{sub}, for the $<\bar{1}10>$- and $<\bar{1}\,\bar{1}2>$-oriented wires. Here, each of the growth thickness is normalized by the growth thickness on a planar substrate, t_{AlGaAs}. As the temperature increased, the growth thickness on the top facets increased, whereas that on the side facets decreased. This is most probably due to the difference in migration and atom incorporation rates between on the top and the side facets. Thus, the growth selectivity, α, is enhanced at higher growth temperatures, as seen in **Fig. 6.**

In **Fig. 4,** the theoretical curves calculated using **Eq. (1)** and the measured growth rate ratio, α, are shown by solid curves. As seen in **Fig. 4**, they showed excellent agreements with the experimental data. Thus, the angle of boundary planes can be kinetically controlled by α, as our model predicts.

Figures 7(a) and (b) summarize the lateral wire width measured as a function of supply thickness of AlGaAs layer, t_{AlGaAs}, just before the start of growth of GaAs QWR. Here, the wire width, w, were normalized by the initial GaAs ridge width, w_0, denoted in **Figs. 2(a) and (b)**. According to our model for evolution of facet boundary planes, w/w_0 should be given by the following equation using the normalized growth rate on the top facet, t_{top}, θ and θ_{top}.

$$\frac{w}{w_0} = 1 - \beta \cdot t_{AlGaAs}, \qquad \beta = 2\frac{t_{top}}{w_0(\tan\theta - \tan\theta_{top})} \tag{2}$$

The straight lines in **Figs. 7(a) and (b)** are those calculated from **Eq. (2)**. Excellent agreement is seen also here, and the wire width, w, can be linearly changed with the value of t_{AlGaAs}, whose sensitivity slope, β, was a function of the growth temperature, T_{sub}.

From these results, it was found that the size of the present QWRs can be kinetically controlled precisely by the growth conditions.

4. Conclusion

Evolution mechanism of heterointerfaces was studied for selective MBE growth of $<\bar{1}10>$- and $<\bar{1}\,\bar{1}2>$-oriented GaAs ridge QWRs on pre-patterned (001) and (111)B substrates. The lateral width of GaAs wires was found to be determined by two facet boundary planes which kept a constant angle, θ, with respect to a flat top pf the mesa pattern. Their evolution turned out to be a kinetic one, reflecting differences in migration and atom incorporation rates on neighboring different facets. Simple formulas derived for θ and wire width showed good agreements with experiments. Thus, the wire width can be controlled precisely by growth conditions.

Acknowledgement

The work reported here is supported in part by 21st Century COE Project at Hokkaido University on "Meme-Media Technology Approach to the R&D of Next-Generation Information Technologies", by Grant-in-Aid for Scientific Research (A)-13305020 and by Grant-in-Aid for Young Scientists (B)-14750223 all from Japanese Government.

References

[1] E. Kapon, D. M. Hwang and R. Bhat: Phys. Rev. Lett., 63 (1989) 430.
[2] T. Fukui, S. Ando, Y. Tokura and T. Toriyama: Appl. Phys. Lett., 58 (1991) 2018.
[3] S. Koshiba, H. Noge, H. Akiyama, T. Inoshita, Y. Nakamura, A. Shimizu, Y. Nagamune, M. Tsuchiya, H. Kano, H. Sakaki and K. Wada: Appl. Phys. Lett., 64 (1994) 363.
[4] X. L. Wang, M. Ogura and H. Matsuhata: Appl. Phys. Lett., 66 (1995) 1506.
[5] H. Fujikura and H. Hasegawa: J. Electron. Mater., 25 (1996) 619.
[6] T. Sato, I. Tamai C. Jiang and H. Hasegawa: Inst. Phys. Conf. Ser., 170-4 (2002) 325.
[7] T. Sato. I. Tamai and H. Hasegawa: presented at ISCS 2002.

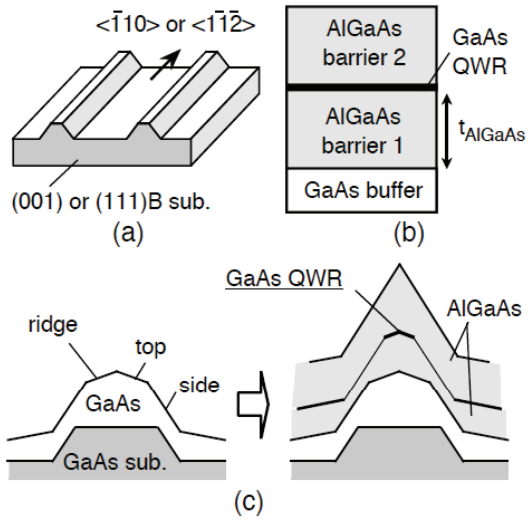

Figure 1: (a) Patterned substrates, (b) material supply and (c) growth sequence.

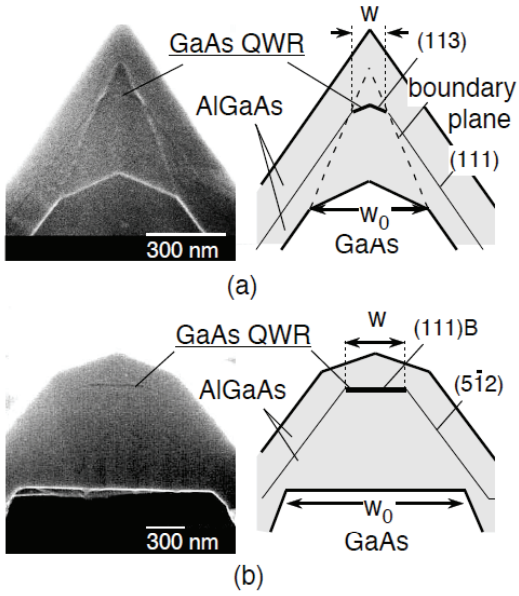

Figure 2: Cross-sectional SEM images of (a) <$\bar{1}$10>-oriented wire and (b) <$\bar{1}\,\bar{1}$2>-oriented wire.

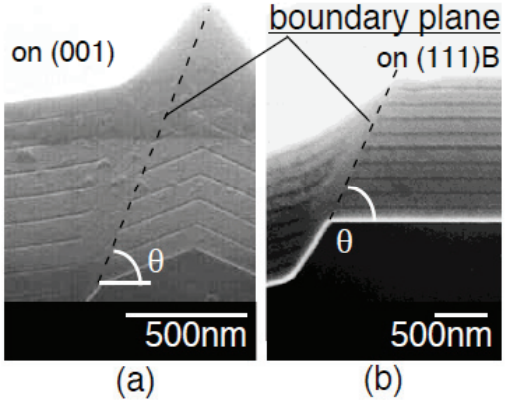

Figure 3: Cross-sectional SEM images of test samples after repeated wires growth (a) on <$\bar{1}$10>-oriented mesa and (b) on <$\bar{1}\,\bar{1}$2>- oriented mesa.

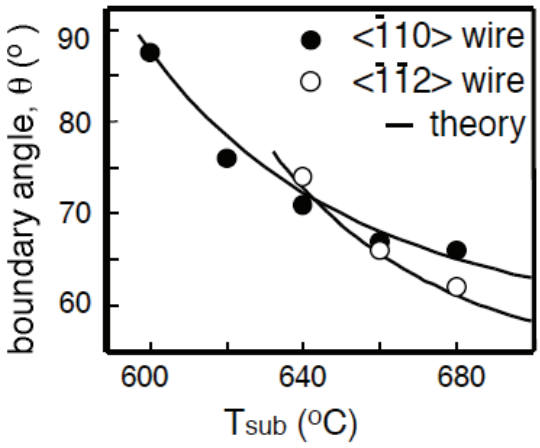

Figure 4: Plots of angle of facet boundary planes vs. substrate temperature.

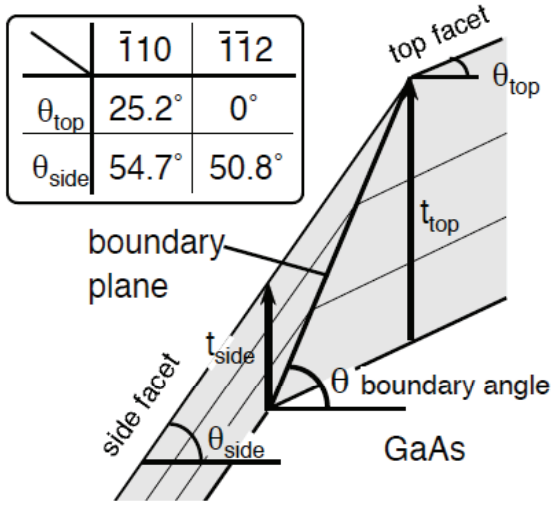

Figure 5: Model for evolution of facet boundary planes.

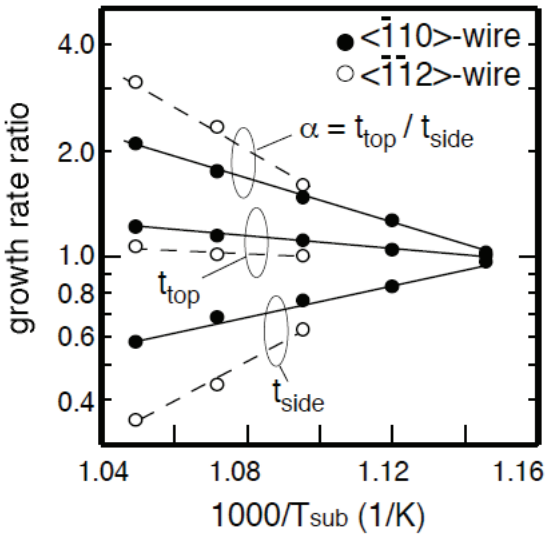

Figure 6: Plots of normalized vertical growth rates vs. substrate temperature.

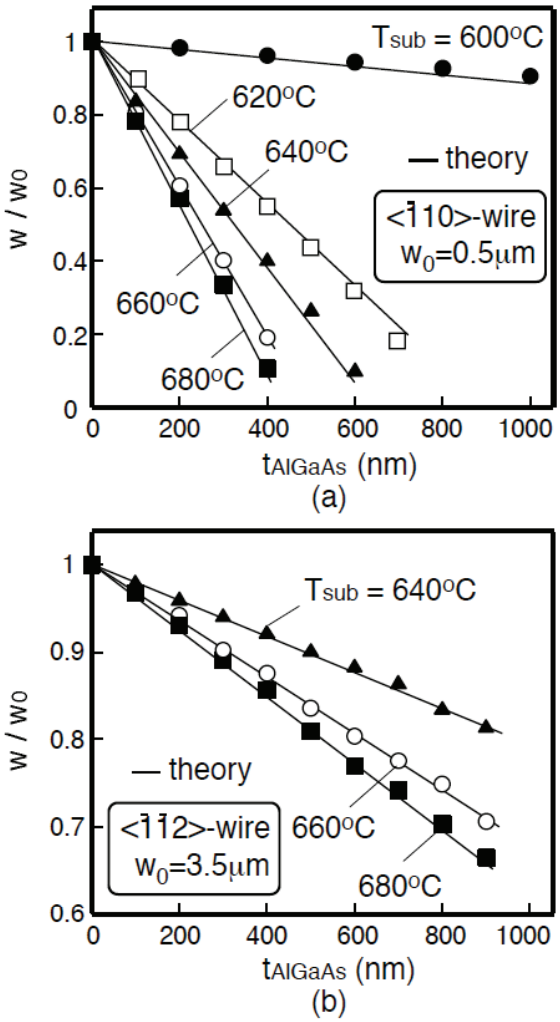

Figure 7: Normalized lateral wire width plotted as a function of the supply thickness of AlGaAs layer for (a) $<\bar{1}10>$-oriented wires and (b) $<\bar{1}\,\bar{1}2>$-oriented wires.